

Asymmetric Hydrogenation. Dimerization of Solvate Complexes: Synthesis and Characterization of Dimeric $[\text{Rh}(\text{DIPAMP})]_2^{2+}$, a Valuable Catalyst Precursor

Angelika Preetz,[†] Wolfgang Baumann,[†] Christian Fischer,[†] Hans-Joachim Drexler,[†]
Thomas Schmidt,[‡] Richard Thede,[‡] and Detlef Heller^{*†}

[†]Leibniz Institute for Catalysis at the University of Rostock, Albert-Einstein-Strasse 29A, D-18059 Rostock, Germany, and [‡]Institute for Biochemistry, Felix-Hausdorff-Strasse 4, D-17489 Greifswald, Germany

Received December 19, 2008

The hydrogenation of $[\text{Rh}(\text{DIPAMP})(\text{NBD})]\text{BF}_4$ (DIPAMP = 1,2-bis[(2-methoxyphenyl)(phenylphosphino)]ethane, NBD = 2,5-norbornadiene) in methanol leads not only to the formation of the expected solvate complex $[\text{Rh}(\text{DIPAMP})(\text{MeOH})_2]\text{BF}_4$ but also to the arene-bridged dimeric species $[\text{Rh}(\text{DIPAMP})]_2(\text{BF}_4)_2$. The dimer is characterized by X-ray analysis as well as by an extensive NMR solution study including ¹H, ³¹P, and ¹⁰³Rh NMR. When used as a precursor for the asymmetric hydrogenation of prochiral olefins, $[\text{Rh}(\text{DIPAMP})]_2(\text{BF}_4)_2$ operates without induction periods. It can be used for the formation of catalyst–substrate complexes such as $[\text{Rh}(\text{DIPAMP})(\text{MAC})]\text{BF}_4$ (MAC = methyl (*Z*)- α -acetamidocinnamate).

Introduction

In want of superior precatalysts for homogeneous catalysis, the existence of dimeric rhodium-arene complexes with diphosphines has been proven several times. Halpern et al. were the first to describe the dimerization of the solvate complex $[\text{Rh}(\text{DPPE})(\text{MeOH})_2]\text{BF}_4$ (DPPE = 1,2-bis(diphenylphosphino)ethane) to yield $[\text{Rh}(\text{DPPE})]_2^{2+}$ (**1**), in which each Rh atom is bonded to two P atoms of a DPPE ligand and through π -arene coordination to a phenyl ring of the DPPE ligand of the second Rh atom.^{1,2} Further investigations on the DPPE system as precatalyst for homogeneous hydroacylation were carried out by Bosnich et al.³ An extensive NMR solution study of the CYCPHOS (CYCPHOS = 1,2-bis(diphenylphosphino)-1-cyclohexylethane) system was elaborated by Riley.⁴ Other systems containing dimeric Rh-diphosphine species have been observed;⁵ however, so far the DPPE ligand remains the only diphosphine of which crystals of the dimeric Rh species could

be analyzed by X-ray. Dimeric Rh-arene complexes with monodentate P-ligands are reported as well.⁶ This work will present the first X-ray structure and a detailed NMR solution study of the dimeric Rh-arene complex with the chiral ligand DIPAMP (DIPAMP = 1,2-bis[(2-methoxyphenyl)(phenylphosphino)]ethane).

The DIPAMP⁷ ligand is one example of the successful application of homogeneous catalysis on an industrial scale⁸ that has also experienced wide mechanistic investigations from an academic viewpoint.⁹ The transformation of diolefin complexes $[\text{Rh}(\text{DIPAMP})(\text{diolefin})]^+$ (diolefin = NBD (**2**,

*Corresponding author. E-mail: detlef.heller@catalysis.de.

(1) (a) Halpern, J.; Riley, D. P.; Chan, A. S.; Pluth, J. J. *J. Am. Chem. Soc.* **1977**, *99*, 8055–8057. (b) For the influence of arene complexes on the catalytic activity of asymmetric hydrogenations see: Heller, D.; Drexler, H.-J.; Spannenberg, A.; Heller, B.; You, J.; Baumann, W. *Angew. Chem., Int. Ed.* **2002**, *41*, 777–780.

(2) Halpern's X-ray structure of the DPPE dimer was not deposited in the Cambridge database. A new X-ray crystal structure of the DPPE dimer **1** is included in the Supporting Information, Figure S1, of this work.

(3) (a) Barnhart, R. W.; Wang, X.; Noheda, P.; Bergens, S. H.; Whelan, J.; Bosnich, B. *Tetrahedron* **1994**, *50*, 4335–4346. (b) Fairlie, D. P.; Bosnich, B. *Organometallics* **1988**, *7*, 946–954, and on the DPPP, DPPB, and CHIRAPHOS. (c) Bergens, S. H.; Noheda, P.; Whelan, J.; Bosnich, B. *J. Am. Chem. Soc.* **1992**, *114*, 2121–2128. (d) Fairlie, D. P.; Bosnich, B. *Organometallics* **1988**, *7*, 936–945.

(4) Riley, D. P. *J. Organomet. Chem.* **1982**, *234*, 85–97.

(5) BINAP: (a) Miyashita, A.; Takaya, H.; Souchi, T.; Noyori, R. *Tetrahedron* **1984**, *8*, 1245–1253. (b) Miyashita, A.; Yasuda, A.; Takaya, H.; Toriumi, K.; Noyori, R. *J. Am. Chem. Soc.* **1980**, *102*, 7932–7934. (c) DIPH: Allen, D. G.; Wild, S. B.; Wood, D. L. *Organometallics* **1986**, *5*, 1009–1015. (d) SKEWPHOS: Mikami, K.; Yusa, Y.; Hatano, M.; Wakabayashi, K.; Aikawa, K. *Chem. Commun.* **2004**, 98–99. (e) BIPHEP: Mikami, K.; Kataoka, S.; Yusa, Y.; Aikawa, K. *Org. Lett.* **2004**, *6*, 3699–3701.

(6) (a) PPh₃: Rifat, A.; Patmore, N. J.; Mahon, M. F.; Weller, A. S. *Organometallics* **2002**, *21*, 2856–2865. (b) Marcuzzan, P.; Ezhova, M. B.; Patrick, B. O.; James, B. R. *C. R. Chim.* **2002**, *5*, 373–378. (c) BINAP-THOXO: Gridnev, I. D.; Fan, C.; Pringle, P. G. *Chem. Commun.* **2007**, 1319–1321. (d) For redox-switchable ligand, see for example: Singewald, E. T.; Mirkin, C. A.; Stern, C. L. *Angew. Chem., Int. Ed. Engl.* **1995**, *35*, 1624–1627.

(7) Vineyard, B. D.; Knowles, W. S.; Sabacky, M. J.; Bachman, G. L.; Weinkauff, D. J. *J. Am. Chem. Soc.* **1977**, *99*, 5946–5952.

(8) Knowles, W. S. *Asymmetric Hydrogenation—The Monsanto L-Dopa Process*. In *Asymmetric Catalysis on Industrial Scale*; Blaser, H. U., Schmidt, E., Eds.; Wiley-VCH: New York, 2004; Chapter 1.1, pp 23–53.

(9) (a) Schmidt, T.; Drexler, Sun, A.; Dai, Z.; Baumann; Preetz, A. *Adv. Synth. Catal.* **2009**, *351*, 750–754. (b) Preetz, A.; Baumann, W.; Drexler, H.-J.; Fischer, C.; Sun, J.; Spannenberg, A.; Zimmer, O.; Hell, W.; Heller, D. *Chem. Asian J.* **2008**, *3*, 1979–1982. (c) Schmidt, T.; Dai, Z.; Drexler, H.-J.; Baumann, W.; Jäger, C.; Pfeifer, D.; Heller, D. *Chem.—Eur. J.* **2008**, *14*, 4469–4471. (d) Gridnev, I. D.; Imamoto, T.; Hoge, G.; Kouchi, M.; Takahashi, H. *J. Am. Chem. Soc.* **2008**, *130*, 2560–2572. (e) Drexler, H.-J.; Baumann, W.; Schmidt, T.; Zhang, S.; Sun, A.; Spannenberg, A.; Fischer, C.; Buschmann, H.; Heller, D. *Angew. Chem., Int. Ed.* **2005**, *44*, 1184–1188. (f) Wada, Y.; Imamoto, T.; Tsuruta, H.; Yamaguchi, K.; Gridnev, I. D. *Adv. Synth. Catal.* **2004**, *346*, 777–788. (g) Schmidt, T.; Baumann, W.; Drexler, H.-J.; Arrieta, A.; Buschmann, H.; Heller, D. *Organometallics* **2005**, *24*, 3842–3848. (h) McCulloch, B.; Halpern, J.; Thomas, M. R.; Landis, C. R. *Organometallics* **1990**, *9*, 1392–1395. (i) Landis, C. R.; Halpern, J. *J. Am. Chem. Soc.* **1987**, *109*, 1746–1754. (j) Brown, J. M.; Parker, D. J. *Org. Chem.* **1982**, *47*, 2722–2730. (k) Brown, J. M.; Chaloner, P. A. *J. Chem. Soc., Chem. Commun.* **1980**, 344–346. (l) Brown, J. M.; Chaloner, P. A. *J. Am. Chem. Soc.* **1980**, *102*, 3040–3048. (m) Brown, J. M.; Chaloner, P. A. *Tetrahedron Lett.* **1978**, *21*, 1877–1881.

Table 1. Pseudo-First-Order Rate Constants k'_{NBD} for the NBD Hydrogenation of $[\text{Rh}(\text{DIPAMP})(\text{NBD})]\text{BF}_4$ in Different Solvents

solvent	k'_{NBD} in min^{-1}
MeOH	ca. 9
EtOH	13.2
<i>i</i> -PrOH	5.9
THF	5.0
trifluoroethanol	3.9
propylene carbonate	4.8

5-norbornadiene), COD (1,5-cyclooctadiene)) into the solvate complex $[\text{Rh}(\text{DIPAMP})(\text{MeOH})_2]^+$ has been investigated qualitatively by the groups of Halpern and Brown.^{9i,9l,9m}

Results and Discussion

The determination of pseudo-first-order rate constants for the hydrogenation of several diolefin complexes of the type $[\text{Rh}(\text{PP})(\text{diolefin})]^+$ (PP = diphosphine) to the respective solvate complexes under isobaric conditions has been described in detail.¹⁰

Applying the hydrogenation technique elaborately described in ref 11, pseudo-first-order rate constants ($k'_{\text{NBD}} = k_{\text{NBD}} \times [\text{H}_2]$) result for the hydrogenation of $[\text{Rh}(\text{DIPAMP})(\text{NBD})]\text{BF}_4$ in MeOH, EtOH, THF, *i*-PrOH, trifluoroethanol, and propylene carbonate as summarized in Table 1; see also Supporting Information, Figures S2, S3.

The time for complete removal of NBD in the precatalyst can be calculated from the 7-fold half-life $t_{1/2}$ for the pseudo-first-order reaction ($t_{1/2} = \ln 2/k'$), which corresponds to ca. 99.2% conversion of NBD. After this time practically no more signals of diolefin complex $[\text{Rh}(\text{DIPAMP})(\text{NBD})]\text{BF}_4$ should be detectable in the ³¹P NMR spectrum. To verify the results, $[\text{Rh}(\text{DIPAMP})(\text{NBD})]\text{BF}_4$ was hydrogenated in the respective solvents for the time calculated from k' values. In all the cases, signals of the diolefin complexes were no longer detectable; see Supporting Information, Figures S4–S9.

Independent of the solvent, the stoichiometric hydrogenation of NBD in $[\text{Rh}(\text{DIPAMP})(\text{NBD})]^+$ is remarkably faster than the hydrogenation of COD in $[\text{Rh}(\text{DIPAMP})(\text{COD})]\text{BF}_4$ in MeOH, a fact that has been known for some time.^{9l,9m}

A different approach to determine pseudo rate constants is opened up by UV/vis spectroscopy. While for the cases shown above *catalytic* hydrogenations were monitored by hydrogen consumption, here *stoichiometric* hydrogenations can be followed. This method is especially suitable for very slow hydrogenations. In ref 10a application of UV/vis spectroscopy was introduced for the determination of the pseudo rate constant k' for the hydrogenation of $[\text{Rh}(\text{DPPE})(\text{COD})]\text{BF}_4$ in MeOH ($k' = 0.0033 \text{ min}^{-1}$).

The reaction spectrum for the stoichiometric hydrogenation of COD in $[\text{Rh}(\text{DIPAMP})(\text{COD})]\text{BF}_4$ in MeOH is exhibited in Figure 1. In principle, two isosbestic points are visible at 416 and 459 nm. However, the one at 416 nm is not

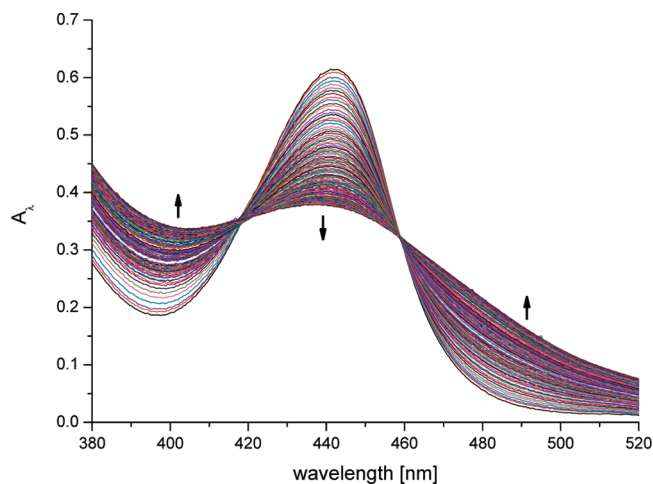


Figure 1. UV/vis reaction spectrum for the stoichiometric hydrogenation of $[\text{Rh}(\text{DIPAMP})(\text{COD})]\text{BF}_4$ (0.008 mmol) in 15.0 mL of MeOH at 1.0 bar of total pressure (cycle time 10.0 min, overall time 800 min).

very clear due to the very long reaction time of 800 min. Analysis as a pseudo-first-order reaction with the program SPECFIT (see Supporting Information, Figures S10, S11 contain extinction diagrams and the first-order fit for various wavelengths) gives a pseudo rate constant of 0.0028 min^{-1} (0.0030 min^{-1} for a second measurement), which is even smaller than for the diolefin complex with the achiral ligand DPPE.^{10a}

From the pseudo-first-order rate constant it follows that the complete removal of COD of $[\text{Rh}(\text{DIPAMP})(\text{COD})]\text{BF}_4$ in MeOH at 25 °C and 1 bar of hydrogen pressure takes ca. 27 h, which confirms the difficulties described in refs 9l and 9m.

Hydrogenation of either $[\text{Rh}(\text{DIPAMP})(\text{NBD})]\text{BF}_4$ or $[\text{Rh}(\text{DIPAMP})(\text{COD})]\text{BF}_4$ in MeOH should result in the solvate complex $[\text{Rh}(\text{DIPAMP})(\text{MeOH})_2]\text{BF}_4$ (**2**). The ³¹P NMR spectrum of a solution of $[\text{Rh}(\text{DIPAMP})(\text{MeOH})_2]\text{BF}_4$ gained from the respective NBD complex, however, not only exhibits the doublet expected for such a C_2 -symmetrical ligand but shows further signals (see Supporting Information, Figure S4).¹²

From a highly concentrated solution (0.09 mol/L) of $[\text{Rh}((S,S)\text{-DIPAMP})(\text{MeOH})_2]\text{BF}_4$ orange crystals of $[\text{Rh}((S,S)\text{-DIPAMP})_2]^+$ (**3a**) could be isolated and were analyzed by X-ray, Figure 2, proving a dimeric structure.

This is in analogy with the DPPE dimer **1**, which also precipitates from a highly concentrated solution of the solvate complex. As previously described in the literature for DPPE and other ligands,¹ the structure of **3a** exhibits two rhodium atoms that each coordinate to the chelate ligand and to a phenyl ring of the DIPAMP ligand of the other rhodium atom. The bite angle P–Rh–P (84.2°) does not differ notably from that of the respective $[\text{Rh}(\text{DIPAMP})(\text{NBD})]\text{BF}_4$ (83.6–84.4°) and $[\text{Rh}(\text{DIPAMP})(\text{COD})]\text{BF}_4$ (82.7°) complexes, whereas the Rh–P bond lengths are slightly shortened (2.228 Å versus 2.290–2.312 Å (NBD)

(10) (a) Preetz, A.; Drexler, H.-J.; Fischer, C.; Dai, Z.; Börner, A.; Baumann, W.; Spannenberg, A.; Thede, R.; Heller, D. *Chem.—Eur. J.* **2008**, *14*, 1445–1451, and references therein. (b) Heller, D.; de Vries, A. H. M.; de Vries, J. G. Catalyst Inhibition and Deactivation in Homogeneous Hydrogenation. In *Handbook of Homogeneous Hydrogenation*; de Vries, H. G., Elsevier, C., Eds.; Wiley-VCH: New York, 2007; Chapter 14, pp 1483–1516.

(11) Drexler, H.-J.; Preetz, A.; Schmidt, T.; Heller, D. Kinetics of Homogeneous Hydrogenation: Measurement and Interpretation. In *Handbook of Homogeneous Hydrogenation*; de Vries, H. G., Elsevier, C., Eds.; Wiley-VCH: New York, 2007; Chapter 10, pp 1483–1516.

(12) A similar spectrum is gained in EtOH, *i*-PrOH, and propylene carbonate, whereas in THF and trifluoroethanol there are no more signals of a solvate complex observable, but only the unknown signals; see Supporting Information, Figures S5–S9. In the ³¹P NMR spectrum of $[\text{Rh}(\text{DIPAMP})(\text{MeOH})_2]\text{BF}_4$, with the widely investigated dimethyl itaconate (Rh:substrate = 1:1), the same signals are visible, which were then left unidentified; see Supporting Information, Figure S12 and ref 9c.

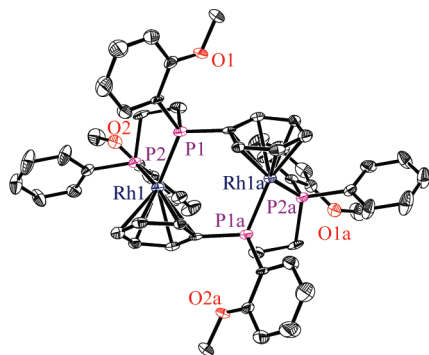


Figure 2. X-ray structure of the cation in $[\text{Rh}((S,S)\text{-DIPAMP})_2(\text{BF}_4)_2 \cdot \text{MeOH}]$ (**3a**) (ORTEP, 30% probability ellipsoids). Hydrogen atoms and the MeOH molecule are omitted for clarity. Selected distances [Å] and angles [deg]: $\text{Rh1}-\text{Rh1a} = 4.144$, $\text{Rh1}-\text{P1} = 2.221(2)$, $\text{Rh1}-\text{P2} = 2.228(2)$, $\text{Rh1}-\text{C} = 2.258\text{--}2.346(8)$, Rh1 –centroid of phenyl rings = 1.843, $\text{P1}-\text{Rh1}-\text{P2} = 84.2(1)$.

and 2.282 Å (COD)).¹³ Redissolving the crystals of **3a** in CD_3OD reproduces the ^{31}P NMR spectrum gained by hydrogenation of $[\text{Rh}(\text{DIPAMP})(\text{NBD})]\text{BF}_4$ in CD_3OD . From the respective ^1H NMR spectrum one can deduce that there must be at least one other species in solution beside the solvate complex and **3a**. Both **3a** and the third species exhibit high-field protons characteristic for arene bridges.^{1,5,6} With the structure of the DIPAMP ligand in mind other structural motifs can be considered to be in equilibrium with the phenyl–phenyl-bridged one (**3a**) that was crystallized. First, an *o*-anisyl-*o*-anisyl-bridged symmetric species is possible, and second, an unsymmetrical species in which one phenyl and one *o*-anisyl ring establish the arene bridge is possible.

To identify the signals of the isolated crystals with the phenyl–phenyl structure **3a**, single crystals were dissolved at -80 °C to freeze out any equilibrium to other possible dimeric species.^{9c} The solvent was changed to relatively noncoordinating dichloromethane (CD_2Cl_2) due to the low solubility of **3a** in MeOH at low temperature and owing to the low concentration of **3a** and the additional species in $\text{MeOH}-d_4$ (equilibrium to the solvate complex in MeOH).

Accordingly, low-temperature NMR of **3a** in CD_2Cl_2 afforded spectra of pure **3a**. The ^1H NMR spectrum in CD_2Cl_2 at 213 K shows three characteristic high-field protons at 5.4, 6.1, and 6.5 ppm, which can be attributed to protons of the phenyl ring of the DIPAMP ligand that interact with a rhodium atom; see Supporting Information, Figures S13–S17. In the ^{31}P NMR of **3a** at 213 K two signal sets are visible: the one at 83 ppm showing four lines, the one at 73 ppm broadened but probably four lines as well. Gentle heating of the sample resulted in a slight upfield shift and resolution of a complicated fine structure. Due to the higher order of the spin system consisting of four ^{31}P and two ^{103}Rh nuclei (AA'BB'XX'), there are clearly more than the eight lines one would expect for a mononuclear C_1 -symmetric rhodium complex (ABX system). Not until a temperature higher than 0 °C is reached do additional signals appear. ^1H NMR proves an additional species in solution that must be unsymmetrical (four instead of two methoxy resonances). $^1\text{H}-^1\text{H}$ COSY NMR of the equilibrated solution confirms

that five protons of a phenyl bridge and four protons of an *o*-anisyl bridge can be found with high-field shifts of up to 4.3 ppm; see Supporting Information, Figures S18, S19. Thus, the second species in solution is the unsymmetrical dimeric species in which one phenyl and one *o*-anisyl ring establish the arene bridge (**3b**). Dissolving single crystals of **3a** in CD_3OD at -30 °C revealed that already at this low temperature the equilibrium between the two dimeric species **3a** and **3b** was established.¹⁴

Further analysis of the NMR spectra was accomplished by shift correlation experiments including both $^{31}\text{P}-^{103}\text{Rh}$ and $^1\text{H}-^{103}\text{Rh}$ HMQC NMR (Figure 3) as well as $^1\text{H}-^{31}\text{P}$ HMQC NMR (Figure S20). We find three different rhodium environments. Correlation with the ^{31}P NMR of **3a** reveals that the signal at -837 ppm belongs to symmetrical dimer **3a**, Figure 3 (top). The other two signals at -822 and -766 ppm¹⁵ are both assigned to unsymmetrical **3b**, thus confirming the interpretation of the ^1H NMR. Figure 3 (bottom) clearly shows the correlation of three of the arene bridging protons to the respective rhodium cores.

As low-temperature NMR experiments have shown in CD_2Cl_2 , the two dimeric species **3a** and **3b** are in equilibrium; that is, they can interconvert. In MeOH equilibration can additionally be obtained via the solvate complex **2**; dissolution of single crystals of **3a** leads to a mixture of **2**, **3a**, and **3b**. These experimental findings lead to the reaction sequence shown in Scheme 1.

At ambient temperature equilibration between dimers **3a** and **3b** is fast; already 1 min after dissolution of **3a** in CD_2Cl_2 the UV/vis spectrum is constant. In $\text{MeOH}-d_4$ in the ^{31}P NMR spectrum both dimers **3a** and **3b** can be detected besides the solvate complex **2**. The ratio of dimers **3a** and **3b** is constant, independent of the initial concentration (dilution) of **3a**.

Thus, from the NMR spectra equilibrium constants for the formation of the dimeric species can be determined. The gross stability constant as the sum of the individual stability constants is calculated according to eq 1.

$$K_{\text{gross}} = \frac{[\mathbf{3a}] + [\mathbf{3b}]}{[\mathbf{2}]^2} = K_{\mathbf{3a}} + K_{\mathbf{3b}} \quad (1)$$

The ratio of individual stability constants ($K_{\mathbf{3a}}/K_{\mathbf{3b}}$) directly corresponds to the concentration ratio of the two dimers $[\mathbf{3a}]/[\mathbf{3b}]$.

For the determination of concentrations of the solvate complex and the dimers, ^1H NMR data (signals of the methoxy groups of the ligand) were used. In addition, the signals of the protons establishing the arene bridge can be used for verification of the ratio of $[\mathbf{3a}]/[\mathbf{3b}]$, Supporting Information, Figure S22.¹⁶

Four measurements result in an average gross stability constant of 52 L/mol and stability constants of 34 L/mol for **3a** and 18 L/mol for **3b**. Hence, the phenyl–phenyl-bridged dimer is twice as stable as the phenyl-*o*-anisyl-bridged one. Those stability constants are consistent with values reported by Halpern et al. for $[\text{Rh}(\text{DPPE})(\text{benzene})]^+$ (18 L/mol) and $[\text{Rh}(\text{DPPE})(\text{toluene})]^+$ (97 L/mol).^{1a}

(14) This temperature was chosen owing to the high viscosity of MeOH and to the low solubility of **1** in MeOH at lower temperatures.

(15) The chemical shifts are in the range of known values for rhodium DIPAMP arene complexes, e.g., $[\text{Rh}(\text{DIPAMP}(p\text{-xylene}))\text{BF}_4]$ with -956 ppm and $[\text{Rh}(\text{DIPAMP})(\text{benzene})\text{BF}_4]$ with -1006 ppm; see ref 1b.

(16) ^{31}P NMR data are not suitable due to the fact that signals of all species overlap.

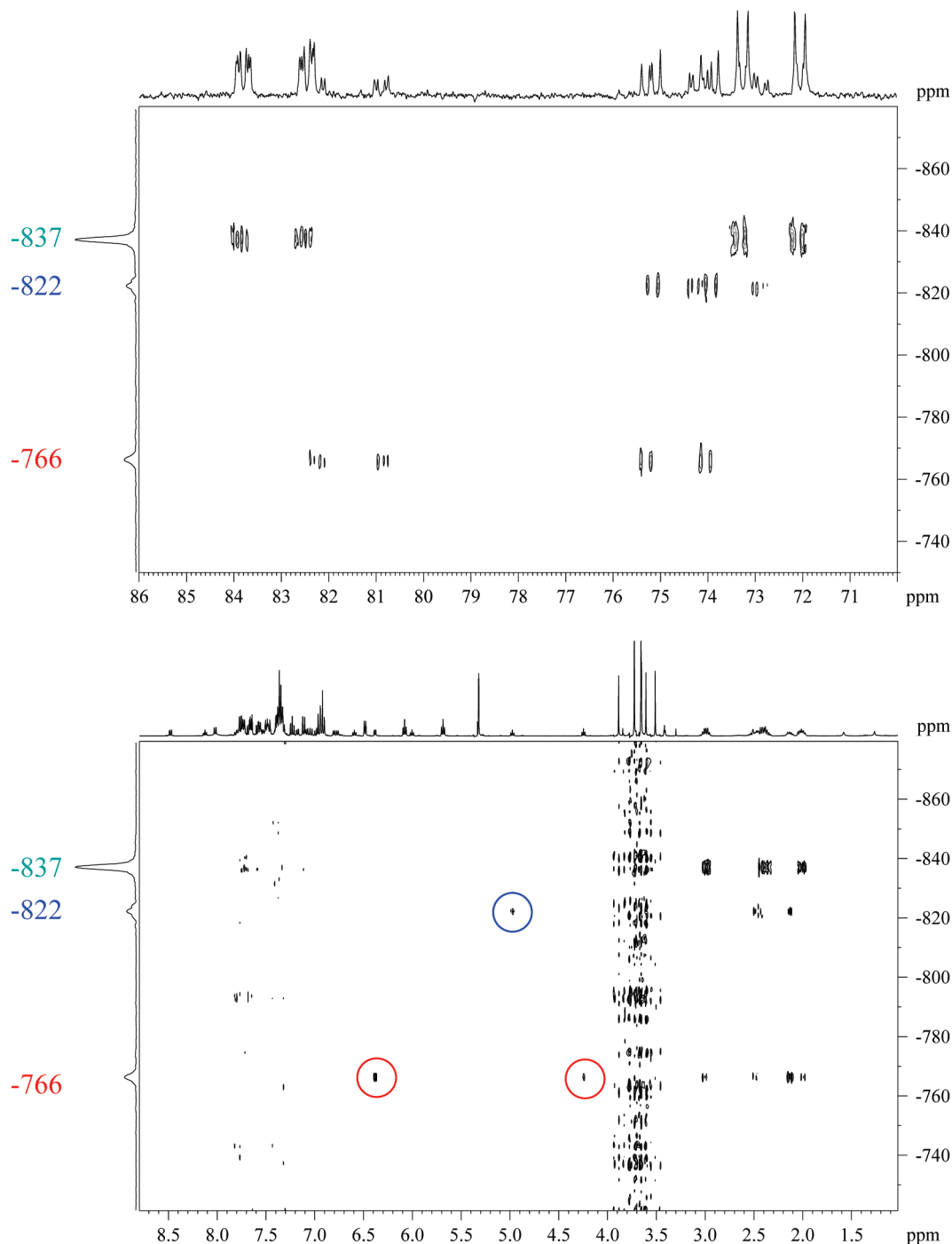


Figure 3. $^{31}\text{P}-^{103}\text{Rh}\{^1\text{H}\}$ (top) and $^1\text{H}-^{103}\text{Rh}\{^{31}\text{P}\}$ (bottom) HMQC NMR spectra of $[\text{Rh}(\text{DIPAMP})]_2(\text{BF}_4)_2$ (**3**) in CD_2Cl_2 (298 K): mixture of **3a** [$\delta(^{103}\text{Rh}) -837$ ppm] and **3b** [$\delta(^{103}\text{Rh}) -822$ and -766 ppm]. The signals encircled are due to η^6 -coordinated arenes. Further details on acquisition and interpretation of these spectra are provided in the Supporting Information, Figure S21.

To demonstrate the applicability of the dimers **1** and **3** as precatalysts, they were used in the asymmetric hydrogenation of (*Z*)- α -acetamidocinnamic acid and methyl (*Z*)- α -acetamidocinnamate (MAC). In Figure 4 the hydrogen consumption is shown in comparison to that in which the solvate complex $[\text{Rh}(\text{PP})(\text{MeOH})_2]\text{BF}_4$ was prepared *in situ* and used as catalyst. Within the range of reproducibility the hydrogenations result in the same activity (and enantioselectivity for the chiral ligand DIPAMP, 96% ee) under identical conditions and in that agree well with the literature data of ref 9i. Obviously, the catalyst–substrate complexes are

rapidly formed from the respective dimer and the substrate in solution.

The hydrogenation of MAC with the Rh/DIPAMP system is one of the most widely investigated enantioselective hydrogenations.⁹ⁱ Although the diastereomeric catalyst–substrate complexes exhibit a high thermodynamic stability, a catalyst–substrate complex could not yet be characterized by X-ray analysis. Apparently, the substrate complexes are too soluble in the applied solvent methanol.

Here, the dimeric species **3a** offers an alternative approach. Due to the fact that **3a** already precipitates during the

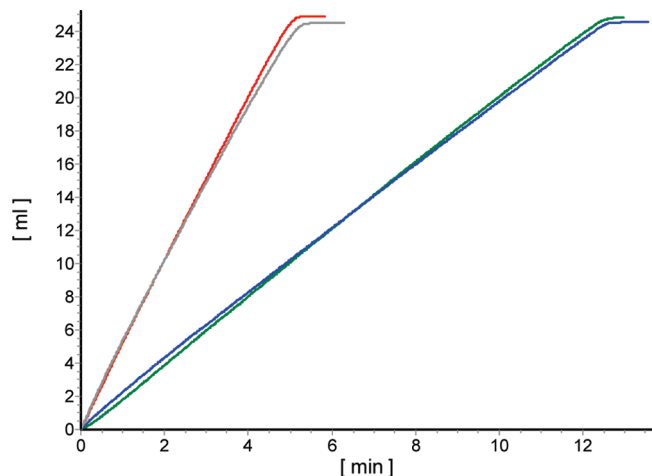


Figure 4. Comparison of the asymmetric hydrogenation of (*Z*)- α -acetamidocinnamic acid with $[\text{Rh}(\text{DPPE})(\text{MeOH})_2]\text{BF}_4$ (red) and **1** (gray) and of MAC with $[\text{Rh}((S,S)\text{-DIPAMP})(\text{MeOH})_2]\text{BF}_4$ (green) and (*S,S*)-**3a** (blue). Conditions: 0.01 mmol of Rh; 1.0 mmol of prochiral olefin; 15.0 mL of MeOH; 25.0 °C; 1 bar of total pressure.

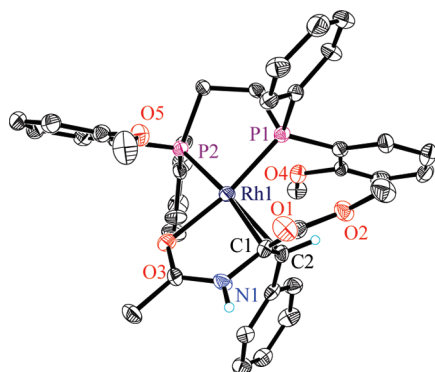
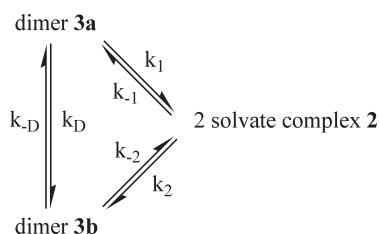


Figure 5. X-ray structure of the cation in $[\text{Rh}((R,R)\text{-DIPAMP})(\text{MAC})]\text{BF}_4$, **4** (ORTEP, 30% probability ellipsoids). Hydrogen atoms except on C2 and N1 are omitted for clarity. Selected distances [Å] and angles [deg]: Rh1–O3 = 2.092(5); Rh–C1 = 2.164(5); Rh–C2 = 2.162(6); Rh–P1 = 2.230(2); Rh–P2 = 2.300(2); P1–Rh–P2 = 82.7(1).

Scheme 1. Reaction Sequence for the Equilibria between Species 2, 3a, and 3b



hydrogenation of $[\text{Rh}(\text{DIPAMP})(\text{NBD})]\text{BF}_4$ in *i*-PrOH owing to its very low solubility, the isolation of catalyst–substrate complexes seemed possible. Indeed, single crystals suitable for X-ray crystallography were grown by layering a solution of **3a** and MAC in *i*-PrOH (Rh:substrate = 1:5) with diethyl ether, yielding $[\text{Rh}((R,R)\text{-DIPAMP})(\text{MAC})]\text{BF}_4$, **4**, Figure 5.

The substrate coordinates via the C–C double bond and the oxygen of the acetyl group to the Rh. This is in accordance

with the expected coordination mode already observed for other dehydroamino acid derivatives^{9c,9g,9h} and dimethyl itaconate^{9c} with DIPAMP as ligand.

The addition of hydrogen from the rhodium site to the coordinating substrate would formally lead to the (*R*) product. The enantioselective hydrogenation of MAC in MeOH at 25 °C under normal pressure with the (*R,R*)-DIPAMP catalyst, however, yields the (*S*)-product in enantiomeric excess (ee = 96%). Obviously, the isolated crystal corresponds to the major substrate complex, which does not lead to the main enantiomer. Hence, this result is a supplementary confirmation of the milestone work of Landis and Halpern, who derived this well-known major-minor-principle mainly from kinetic investigations.⁹ⁱ

Experimental Section

All experiments were carried out under an argon atmosphere using standard Schlenk techniques. NMR spectra were recorded with a Bruker AV 400 NMR spectrometer. UV/vis spectra were measured with a Lambda 19 (Perkin-Elmer).

The general procedure for the catalytic hydrogenation of diolefins and prochiral olefins is described in refs 10 and 11.

$[\text{Rh}(\text{DIPAMP})(\text{solvent})_2]\text{BF}_4$. ³¹P NMR data: CD₃OD, d, δ 81.3 ppm, $J_{\text{P-Rh}}$ 208.1 Hz; EtOH (nondeuterated), d, δ 79.2, $J_{\text{P-Rh}}$ 209.0 Hz; *i*-PrOH-*d*₈, d, δ 77.6, $J_{\text{P-Rh}}$ 210.8 Hz; propylene carbonate (nondeuterated), d, δ 74.1, $J_{\text{P-Rh}}$ 207.2 Hz.

$[\text{Rh}(\text{DIPAMP})_2(\text{BF}_4)_2$ (3**).** $[\text{Rh}(\text{DIPAMP})(\text{NBD})]\text{BF}_4$ (200 mg, 0.27 mmol) was dissolved in 4 mL of MeOH. The flask was purged with hydrogen and the solution stirred. After 20 min the hydrogen was substituted by argon by freezing the solution and subsequent evacuation (3 times). The volume of MeOH was concentrated to approximately 1 mL. An orange precipitate resulted, which was dissolved in the heat. Slow cooling to ambient temperature yielded orange to red crystals that were washed with diethyl ether and dried *in vacuo* (yield of **3**: 134 mg, 76% isolated yield).

3a. ¹H NMR (219 K, in CD₂Cl₂): 7.68–7.51 (10H, m); 7.39–7.34 (2H, m); 7.32–7.29 (8H, m); 7.23 (2H, t, J = 6.5 Hz); 7.15 (2H, t, J = 7.6 Hz); 7.09 (2H, dd, J = 8.3 Hz, 3.9 Hz); 6.92 (2H, dd, J = 8.6 Hz, 2.9 Hz); 6.79 (2H, t, J = 7.3 Hz); 6.49 (2H, t, J = 6.4 Hz); 6.08 (2H, t, J = 6.4 Hz); 5.43 (2H, t, J = 5.6 Hz); 3.76 (6H, s); 3.63 (6H, s); 3.01–2.89 (2H, m); 2.41–2.27 (4H, m); 2.00–1.88 (2H, m); characteristic proton signals at 298 K, 6.48 (2H, t, J = 7.1 Hz, #5); 6.09 (2H, t, J = 6.4 Hz, #2); 5.67 (2H, t, J = 6.4 Hz, #3); 3.71 (6H, s, OCH₃); 3.65 (6H, s, OCH₃). ³¹P NMR (298 K, in CD₂Cl₂): 83.2 ($J_{\text{P-Rh}}$ = 218 Hz, #P1); 72.7 ($J_{\text{P-Rh}}$ = 195 Hz, #P2); labeling refers to Figure S16. ¹⁰³Rh NMR (298 K, in CD₂Cl₂): –837.

3b. ¹H NMR (in CD₂Cl₂): characteristic proton signals at 298 K, 6.60 (1H, t, J = 13.0 Hz, 6.6 Hz, #8); 6.39 (1H, t, J = 6.9 Hz, #6); 6.01 (1H, t, J = 6.2 Hz, #3); 4.98 (1H, t, J = 6.6 Hz, #4); 4.25 (1H, t, J = 5.7 Hz, #7); 3.88 (3H, s, OCH₃); 3.65 (3H, s, OCH₃); 3.61 (3H, s, OCH₃); 3.51 (3H, s, OCH₃) (other signals under those of phenyl–phenyl-bridged dimer). ³¹P NMR (298 K, in CD₂Cl₂): 81.6 ($J_{\text{P-Rh}}$ = 217 Hz); 74.7 ($J_{\text{P-Rh}}$ = 204 Hz); 74.6 ($J_{\text{P-Rh}}$ = 199 Hz); 73.6 ($J_{\text{P-Rh}}$ = 222 Hz); labeling refers to Figure S19. ¹⁰³Rh NMR (298 K, in CD₂Cl₂): –822/–766.

$[\text{Rh}(\text{DIPAMP})(\text{MAC})]\text{BF}_4$ (4**).** $[\text{Rh}(\text{DIPAMP})_2(\text{BF}_4)_2$ (0.01 mmol) and MAC (0.1 mmol) were dissolved in 1 mL of *i*-PrOH, and the solution was subsequently frozen. Diethyl ether (5 mL) was allowed to diffuse into the slowly melting solution, yielding dark red crystals of **4** overnight.

Supporting Information Available: Crystal structure of $[\text{Rh}(\text{DPPE})_2(\text{BF}_4)_2$ (**1**), crystallographic data of **1**, **3a**, and **4**, supportive NMR spectra, extinction diagrams. This material is available free of charge via the Internet at <http://pubs.acs.org>.